THE JOURNAL OF BIOLOGICAL CHEMISTRY VOL. 281, NO. 12, pp. 8254–8263, March 24, 2006

Molecular Cloning and Characterization of UDP-glucose Dehydrogenase from the Amphibian *Xenopus laevis* and Its Involvement in Hyaluronan Synthesis*

Received for publication, August 3, 2005, and in revised form, December 22, 2005 Published, JBC Papers in Press, January 17, 2006, DOI 10.1074/jbc.M508516200

Davide Vigetti[‡], Michela Ori[§], Manuela Viola[‡], Anna Genasetti[‡], Eugenia Karousou[‡], Manuela Rizzi[‡], Francesco Pallotti[‡], Irma Nardi[§], Vincent C. Hascall[¶], Giancarlo De Luca[‡], and Alberto Passi[‡1]

From the [‡]Dipartimento di Scienze Biomediche Sperimentali e Cliniche, Università degli Studi dell'Insubria, via J. H. Dunant 5, 21100 Varese, Italy, [§]Laboratori di Biologia Cellulare e dello Sviluppo, Dipartimento di Fisiologia e Biochimica, Università di Pisa, via Carducci 13, Ghezzano, 56010 Pisa, Italy, and the [¶]Department of Biomedical Engineering and Orthopaedic Research Center/ ND20, The Cleveland Clinic Foundation, Cleveland, Ohio 44195

UDP-glucose dehydrogenase (UGDH) supplies the cell with UDP-glucuronic acid (UDP-GlcUA), a precursor of glycosaminoglycan and proteoglycan synthesis. Here we reported the cloning and the characterization of the UGDH from the amphibian *Xenopus laevis* that is one of the model organisms for developmental biology. We found that *X. laevis* UGDH (xUGDH) maintained a very high degree of similarity with other known UGDH sequences both at the genomic and the protein levels. Also its kinetic parameters are similar to those of UGDH from other species. During *X. laevis* development, UDGH is always expressed but clearly increases its mRNA levels at the tail bud stage (*i.e.* 30 h post-fertilization). This result fits well with our previous observation that hyaluronan, a glycosaminoglycan that is synthesized using UDP-GlcUA and UDP-*N*-acetylglucosamine, is abundantly detected at this developmental stage. The expression of UGDH was found to be related to hyaluronan synthesis. In human smooth muscle cells the overexpression of xUGDH or endogenous abrogation of UGDH modulated hyaluronan synthesis specifically. Our findings were confirmed by *in vivo* experiments where the silencing of xUGDH in *X. laevis* embryos decreased glycosaminoglycan synthesis causing severe embryonic malformations because of a defective gastrulation process.

UDP-glucose dehydrogenase (UGDH,[2] EC 1.1.1.22) catalyzes an NAD^+-dependent, 2-fold oxidation of UDP-glucose (UDP-Glc) to generate UDP-GlcUA (1). In mammals, UDP-GlcUA is used in the biosynthesis of hyaluronan (HA) and the glycosaminoglycans (GAGs) heparan sulfate and chondroitin sulfate (2). In addition, it is used in the liver where glucuronidation targets molecules for excretion (3). UDP-GlcUA also serves as a precursor to UDP-xylose, which provides a major component of the cell wall polysaccharides in plants (4), and represents the initial sugar in GAG synthesis on proteoglycans. In many strains of pathogenic bacteria, such as group A streptoccoci and *Streptococcus pneumoniae* type 3, UDP-GlcUA is used in the construction of the antiphagocytic capsular polysaccharide (5, 6). UGDH is of biochemical mechanistic interest because it belongs to a family of sugar nucleotide-modifying enzymes that catalyze a net four-electron oxidation and serve as both alcohol dehydrogenases and aldehyde dehydrogenases (7).

The importance of UGDH is remarkable considering that its product, UDP-GlcUA, is critical for GAG synthesis. GAG chains of proteoglycans and HA are ubiquitous components of extracellular matrices and pericellular spaces, and an increasing body of information shows the role of GAGs in cell behavior, including signal transduction, cell proliferation, spreading, migration, cancer growth, and metastasis (8–10).

Proteoglycans and HA have important roles throughout the development (11). As UGDH synthesizes UDP-GlcUA, one of the main UDP-sugar precursors, it is not surprising that alteration in UGDH expression causes evident phenotypes in developing embryos, as found by different authors in different model organisms. In particular, in *Drosophila melanogaster* UGDH is encoded by the *sugarless* gene and is required for heparan sulfate modification of proteins that control wing formation (12). In *Caenorhabditis elegans*, UGDH influences GAG synthesis, which is essential for vulval morphogenesis and embryonic development (13, 14). In Zebrafish, the enzyme is critical for normal cardiac development (15). In mouse, UGDH mutants arrest growth during gastrulation with defects in migration of mesoderm and endoderm (16). Moreover, a similar phenotype was found in mutants in the fibroblast growth factor pathway, highlighting that proteoglycans and GAGs facilitate signaling by mammalian growth factors.

Another well known model organism extensively used in developmental biology is the amphibian *Xenopus laevis*. Although several papers report the critical role of proteoglycans in *X. laevis* development (17–22), very limited information is available on GAG functions in amphibian embryogenesis (23–25). Therefore, we have characterized the *X. laevis* UGDH (xUGDH), the key enzyme in GAG biosynthesis in this model organism, as suitable for developmental studies. Here we report the cDNA cloning of xUGDH, its biochemical kinetic parameters, its expression in developing embryos, and its genome organization. We have also extended our observations to *Xenopus tropicalis*, an organism of the same genus as *X. laevis*, but with interesting potential for genetic studies (26). Our results show that the xUGDH expression in human cells increases their HA accumulation (and not that of other GAGs), whereas UGDH abrogation by siRNA reduced HA synthesis and cell-associated GAGs. Moreover, we have also demonstrated that

* This work was supported by MIUR COFIN Project "Analysis of the Hyaluronan-Proteoglycan-Hyaluronan Receptor System in Embryonic Development and Disease" (to D. V.) and Consorzio Interuniversitario Biotecnologie (to A. P.). The costs of publication of this article were defrayed in part by the payment of page charges. This article must therefore be hereby marked "*advertisement*" in accordance with 18 U.S.C. Section 1734 solely to indicate this fact.

The nucleotide sequence(s) reported in this paper has been submitted to the GenBank™/EBI Data Bank with accession number(s) AY762616.

[1] To whom correspondence should be addressed: Dip. di Scienze Biomediche Sperimentali e Cliniche, Università degli Studi dell'Insubria, via J. H. Dunant 5, 21100 Varese, Italy. Tel.: 39-0332-217142; Fax: 39-0332-217119; E-mail: alberto.passi@uninsubria.it.

[2] The abbreviations used are: UGDH, UDP-glucose dehydrogenase; HA, hyaluronan; GAG, glycosaminoglycan; ORF, open reading frame; RT, reverse transcriptase; HAS, HA synthase(s); EST, expressed sequence tag; UTR, untranslated region; MO, morpholino; GFP, green fluorescent protein; FACE, fluorophore-assisted carbohydrate electrophoresis; siRNA, small interfering RNA; xUGDH, *Xenopus* UGDH; AoSMC, aortic smooth muscle cells; IPTG, isopropyl L-D-thiogalactopyranoside; hpf, hours post-fertilization.

UGDH has a crucial role during *X. laevis* development because xUGDH loss of function, by morpholino injection, causes lethal malformation.

MATERIALS AND METHODS

xUGDH Cloning—An *X. laevis* EST data bank was searched for homologies with human UGDH cDNA (GenBank™ accession number NM_003359) using the World Wide Web-based BLAST search engine (www.ncbi.nlm.nih.gov/blast/). IMAGE EST number 4202110 was found and was obtained from MRC geneservice (Cambridge, UK). DNA sequencing was done by an external service facility (BMR, Padua, Italy).

Characterization of the xUGDH Gene—Introns of the *X. laevis xUGDH* gene were amplified with a pair of primers (Table 1) designed on the basis of mouse and human UGDH genomic sequences deposited in public data bases. PCR parameters were as follows: denaturation at 94 °C for 30 s, annealing for 30 s at the temperature indicated in Table 1, and elongation at 72 °C for 5 min for 35 cycles using 1.5 units of La-TAQ (a proofreading DNA polymerase from Takara) following the manufacturer's conditions. Amplification of intron 8 was done using Phusion™ polymerase (Finnzymes) in 6% Me_2SO. PCRs were done on genomic DNA. Amplified intron lengths were determined by gel electrophoresis, and exon/intron boundaries were determined by sequencing the extracted bands from the gels.

In silico determinations of the intron/exon structure of the human, mouse, and *X. tropicalis UGDH* genes were done by BLAST searches on the genomic data bases. Sequence manipulations and contig constructions were done using Vector NTI Suite 6 software.

Recombinant xUGDH Expression and Purification—Cloning and transformation techniques were done essentially as described by Sambrook *et al.* (27). A histidine-tagged xUGDH construct was generated by PCR. Briefly, the xUGDH ORF was amplified using Phusion DNA polymerase (Finnzymes) with the following primers: CCAAGGCTCGAGATGTTTCAGATTAAGAAGATTT and CCTTGGCTCGAGTTAAACTCTTTGTTTCTTATGAGGC (the sequences corresponding to XhoI recognition sites are underlined). The amplified product was digested with XhoI (Takara) and cloned into the XhoI-linearized pET-19b (Novagen) plasmid. This construct (pHisxUGDH) was then sequenced; it encodes the full-length xUGDH protein with an additional His_6 tag sequence at the N terminus.

For protein expression, the plasmid pHisxUGDH was transferred to the host BL21(DE3)pLysS *E. coli* strain (Promega). *E. coli* cells carrying the recombinant plasmid were cultivated at 37 °C in LB medium containing ampicillin and chloramphenicol (100 and 34 μg/ml final concentrations, respectively). After an overnight growth ($A_{600\,nm}$ >2.5), IPTG was added at a final concentration of 1 mM. The temperature was reduced to 30 °C, and the cells were collected after 24 h. Cell extraction and His-tagged xUGDH purification were done using the B-Ter purification kit (Pierce) following the manufacturer's instructions. Some determinations were done on crude extracts that were prepared lysing the bacterial cells in B-Ter solution (Pierce) and recovering the supernatant after centrifugation.

xUGDH Assay—The enzymatic activity of purified His-tagged xUGDH was determined by monitoring the change in absorbance at 340 nm that accompanies reduction of NAD^+ to NADH. The assay conditions were the same as those described previously by Sommer *et al.* (28).

Gene Expression Studies—Total RNA from 21 *X. laevis* embryos (7 from three different females) at different stages of development were extracted using Trizol reagent (Invitrogen) following the manufacturer's protocol. One μg of total RNA from each extract was retrotranscribed using 200 units of Moloney murine leukemia virus reverse transcriptase (Invitrogen) and a $(dT)_{16}$ primer at a concentration of 500 μg/ml. The reaction was done in 50 mM Tris-HCl, pH 8.3, 75 mM KCl, 3 mM $MgCl_2$, 10 mM dithiothreitol, and 500 μM of a dNTP mixture at 42 °C for 50 min. PCR amplifications of the cDNA samples were done using the first strand cDNA synthesis mixture, 25 pmol of primer xUGDH upper primer (CCCTTTGTGAGGCTACAGGA) and xUGDH lower primer (CGGTGCAGATAACCATAGCA), 200 μM dNTPs, and 1 unit of RedTaq polymerase (Sigma) in its own buffer. Reaction mixtures were subjected to eight touchdown cycles with annealing temperatures from 58 to 54 °C and subsequently with cycles using the following parameters: denaturation at 94 °C for 30 s, annealing at 53 °C for 30 s, and elongation at 72 °C for 40 s. As a control for genomic DNA contamination, all reactions were established with the control sample lacking reverse transcriptase. Normalization was done detecting cytoskeletal actin (upper primer, CTGAGTTCATGAAGGATCAC; lower primer, AAATTTACAGGTGTACCTGC) (29) with the above described conditions.

Quantitative real time RT-PCR was used in transfection experiments with aortic smooth muscle cells (AoSMC) (see below). Forty eight hours after transfections, total RNA samples were extracted with Trizol (Invitrogen) and retrotranscribed using the High Capacity cDNA synthesis kit (Applied Biosystems) for 2 h at 37 °C. Quantitative RT-PCR was performed on an ABi Prism 7000 instrument (Applied Biosystems) using the Taqman Universal PCR Master Mix (Applied Biosystems) following the manufacturer's instructions. Probe and primers were developed from TaqMan gene expression assay reagents (Applied Biosystems). The following human TaqMan gene expression assays were used: HAS1 (Hs00155410_m1), HAS2 (Hs00193435_m1), HAS3 (Hs00193436_m1), UGDH (Hs00163365_m1), and β-actin (Hs99999993_m1). Fluorescent signals generated during PCR amplifications were monitored and analyzed with ABi Prism 7000 SDS software (Applied Biosystems). Comparisons of the amounts of each gene transcript among different samples were made using β-actin as a reference. Standard curves were generated by serial dilution of cDNA, and as calculations of PCR efficiency were very similar (about 90%) for each gene assayed, the relative quantitative evaluation of target gene levels was determined by comparing ΔCt (Applied Biosystems user bulletin number 2).

xUGDH Expression in Mammalian Cells—The xUGDH ORF was amplified using Phusion™ DNA polymerase (Finnzymes) with the following primers: TA**CTCGAG**ACCATGTTTCAGATTAAGAAGATTT and AT**CTCGAG**TTAAACTCTTTGTTTCTTATGAGGC. The boldface sequences correspond to XhoI recognition sites, and the underlined adenosine represents the typical −3 purine of the Kozak consensus sequence. The amplified product was purified, A-tailed using RedTaq (Sigma), and cloned into a pTarget (Promega) vector. Expression plasmids were selected to have the insert in the sense orientation to synthesize the complete xUGDH protein (pTarget-xUGDH sense) or to have the insert in the opposite direction used as the control vector (pTarget-xUGDH antisense). DNA sequencing and *in vitro* transcription and translation (TNT *in vitro* transcription/translation system, Promega) were done to check the constructs. AoSMCs (Cambrex) were grown in SmGm2 complete (supplemented with 5% fetal bovine serum) culture medium (Cambrex). The cultures were maintained in an atmosphere of humidified 95% air, 5% CO_2 at 37 °C. 1×10^6 cells between passages 2 and 5 were transiently transfected by means of a Nucleofector apparatus (Amaxa) and the human aortic smooth muscle cells Nucleofector™ kit using 5 μg of either the sense or antisense expression plasmid. After 48 h, transfected cells and conditioned cell culture media were collected. Cells were lysed in 50 mM Tris-HCl, pH 7.4, 150

mM NaCl, 1% Triton X-100 supplemented with a protease inhibition mixture (Roche Applied Science) using a cell scraper. Protein contents in the cell lysates were determined using the Bradford method, and UGDH activities were measured as described above.

Abrogation of Human UGDH—siRNA was used to reduce human UGDH expression in AoSMCs. UGDH siRNA (5′-GGACUAAAA-GAAGUGGUAGGtt-3′) and negative control siRNA 1 kit (scramble, code 4611) were purchased from Ambion. Transfections were done using a Nucleofector apparatus (Amaxa) and the human AoSMC Nucleofector™ kit using an siRNA concentration of 50 μM of either UGDH siRNA or scramble siRNA. After 48 h of incubation, conditioned cell media were assayed for GAG contents by FACE analysis. The transfected cells were used for determination of UDP-sugars contents and UGDH activities. Quantitative real time RT-PCR was used to verify the reduction of UGDH mRNA expression.

GAG Disaccharides and UDP-sugar Precursor Determinations—HA and chondroitin sulfate disaccharides were determined by FACE analysis as described previously (30). UDP-Glc and UDP-GlcUA were quantified by capillary zone electrophoresis using the methodology outlined by Lehmann *et al.* (31). Briefly, 10^6 AoSMCs were lysed in 0.1 ml of phosphate-buffered saline containing 0.5% Triton X-100. After centrifugation, the supernatants were deproteinized by acetonitrile treatment, lyophilized, and resuspended in 90 mM borate buffer, pH 9. Analyses were done using a 75 cm × 50 μm column, 25-kV voltage, and detecting UDP-sugar absorbances at 262 nm. The peak identity was assessed by co-injecting the extracts with commercial UDP-Glc and UDP-GlcUA.

GAG Determinations—To evaluate the amount of each GAG after induction or abrogation of UGDH, AoSMCs were transfected with pTarget-xUGDH constructs or siRNA, respectively, and labeled with [^{3}H]glucosamine (25 μCi/ml) for 48 h in complete SmGm2 medium. Conditioned cell medium was recovered, and the unincorporated [^{3}H]glucosamine was removed by gel filtration using a PD10 column (Amersham Biosciences). The cell layer was washed with phosphate-buffered saline and scraped into 100 μl of phosphate-buffered saline containing 1% Triton X-100, centrifuged at 10,000 × *g* for 10 min at 4 °C. The clear supernatant and the PD10 filtrated medium were digested with proteinase K (Finnzymes) at 50 °C. After 8 h of incubation, proteinase K was inactivated at 90 °C for 10 min. Each GAG solution was separated into 4 aliquots, precipitated by adding 4 volumes of ethanol at −20 °C for 18 h, and recovered by centrifugation. Two aliquots were resuspended in 0.1 M ammonium acetate, pH 7, and digested with 100 milliunits/ml of hyaluronidase SD from *Streptococcus dysgalactiae* (Seikagaku) and 100 milliunits/ml of chondroitinase ABC (Seikagaku), respectively; one was resuspended in 10 mM Tris-HCl, pH 7, 4 mM $CaCl_2$ and digested with 100 milliunits/ml of heparanase I, II, and III (Seikagaku). The last aliquot was used as an undigested control. After 16 h of incubation at 37 °C, which allow complete degradation of 20 μg/ml of standard GAGs, 50 μg of chondroitin sulfate A (Seikagaku) was added to each digested sample as carrier, and undigested GAGs were precipitated with ethanol. Specific GAGs were quantified by counting the radioactivity associated with digestion products (in the supernatant) and the undigested GAGs (pellet) with a liquid scintillation counter (Canberra Packard).

xUGDH Silencing during X. laevis Development—Two antisense morpholino-oligonucleotides (MOs; Gene Tools LLC) were generated on the basis of the xUGDH cDNA sequence, xUGDH MO CATGGT-TTATCTTGCTGAGAACAGA, which is complementary to the xUGDH translation start site and the adjacent coding sequence. A 5-mismatch MO, based on the xUGDH MO sequence, was used as a specificity control (CATcGTTTATgTTGgTGAcAAgAGA, where lowercase letters indicate mismatched nucleotides). The optimal morpholino concentration to inject per embryo was established by independent pilot experiments (not shown) and was determined to be in the range of 10–20 ng/embryo. The MOs were injected bilaterally at the two-cell stage to down-regulate the xUGDH activity in the whole embryo. All the experiments were performed by co-injecting the morpholino-oligonucleotide and the GFP mRNA (300 pg/embryo) as a tracer in order to select only the properly manipulated embryos for the subsequent analysis. Embryos were injected in 0.1× Modified Marc's Ringer solution (MMR) (100 mM NaCl, 1.8 mM KCl, 1 mM $MgCl_2$, 2 mM $CaCl_2$, 5 mM HEPES, pH 7.8) supplemented with 4% Ficoll and then cultured in 0.1× MMR solution until the stage of analysis.

RESULTS AND DISCUSSION

xUGDH cDNA Cloning—In this study we focused our attention on UGDH, a pivotal enzyme in the production of UDP-GlcUA, an important precursor for GAG synthesis. It has been reported that UGDH is crucial in *C. elegans* and *D. melanogaster* morphogenesis (12, 13) and Zebrafish cardiac valve formation (15) and is also involved in mouse gastrulation (16). We reported previously the characterization of HA synthases (HAS1, HAS2, and HAS3) in *X. laevis* and showed their regulation during the early stages of development (34, 35). It is also possible that UGDH, which provides one of the substrates for HAS, is regulated in the embryogenesis of this species. Therefore, we decided to clone *X. laevis* UGDH and characterize it.

To obtain the sequence of the xUGDH mRNA, we initially performed a BLAST search using the human UGDH sequence against an *X. laevis* EST data base. This revealed several ESTs with a high degree of identity with the human sequences. We then obtained the largest EST (dbEST code 4202110) from MRC geneservice (Cambridge, UK); we completed the sequence and deposited in the public data base with GenBank™ accession number AY762616 (data not shown). This sequence has a 42-bp-long 5′-UTR and a 1482-bp-long ORF coding for a protein with 494 amino acids, a calculated molecular mass of 55,209.4 Da, and a calculated isoelectric point of 6.49. A PROSITE analysis (www.expasy.org/prosite/) and a NetPhos analysis (www.cbs.dtu.dk/services/NetPhos/) of the xUGDH amino acid sequence revealed several putative phosphorylation sites. Although we did not further investigate the possibility of post-translation modifications in this enzyme, previous studies have reported that UGDH may be phosphorylated in prokaryotic cells (36, 37).

We searched for known signal peptides using the PSORT II program (www.psort.org/) without identifying any sorting sequence. xUGDH localization was predicted to be cytoplasmic with a 65.2% probability. Such a localization is consistent with a previous report that placed UGDH in the cytosol (13).

The deduced amino acid sequences of xUGDH and other known UGDH from several species are aligned (data not shown). The N-terminal region has the consensus sequence for NAD binding (*i.e.* G*X*G*XX*G) that is maintained with a high degree of identity among all the UGDH analyzed. The central region of the protein (*i.e.* GFGGSCFQKDVLN) has been proposed to be the catalytic domain (38), and all the aligned sequences show a high degree of identity with only a minor amino acid substitution in the UGDH belonging to *C. elegans*, *D. melanogaster*, and soybean. Moreover, the critical cysteine residue, number 276 of xUGDH, is conserved in all sequences, and it has been shown to be involved during the second half-reaction of UGDH (*i.e.* conversion of UDP-aldehydroglucose to UDP-GlcUA) (28). With respect to function/structure considerations, proline residues at positions 92 and 160 are believed to represent main bends in the protein structure (39–41), and they are conserved for UGDH

TABLE 1
Sequence of the primers used in this work to amplify the indicated intron

Intron	Primer	Sequence 5′–3′	Annealing temperature °C
Intron 1	XEso1_up	CGTGATTGCCCAAATGTGTC	53
	XEso2_low	CAGCTTCCTGTATAGCTCCGTCT	
Intron 2	XEso2_up	GCCGAGGCAAGAATCTGTTT	52
	XEso3_low	ATCAAATATCCGCCGAATGC	
Intron 3	XEso3_up	TGCCAGAAGGATTGTCCAAA	53
	XEso4_low	TCACATAGTGCACGCACAGC	
Intron 4	XEso4_up	ACCGGGTGTTAATTGGTGGA	53
	XEso5_low	TTCCTCCACATCTGCTCCTG	
Intron 5	XEso5_up	ATGCTTTCCTTGCCCAGAGA	53
	XEso6_low	TTGCCACTTCATGCAGGTTC	
Intron 6	XEso6_up	GCTGTTTCCAAAAGGATGTCTTG	53
	XEso7_low	TGCAAAACCAAGGAGAGCAA	
Intron 7	XEso7_up	CAAGGATTATCGATTGCCTGTT	53
	XEso8_low	CCCTTGGAACTTTGGGATCA	
Intron 8	XEso8_up	CCTCATGGATGAAGGTGCAA	54
	XEso9_low	CCATTCGGTGCAGATAACCA	
Intron 9	XEso9_up	GCTGGTTCACATTTCTACGGATT	53
	XEso10_low	TATTTTGCAGCTCGCCATGA	
Intron 10	XEso10_up	AGAATGATGTTGAAGCCAGCA	53
	XEso11_low	GCAGGTCTTGCAAACCGAAT	

from all species. Two lysine residues at positions 220 and 339 are also conserved, which correspond to lysine 219 and 338 of bovine UGDH. One of these lysine residues is probably catalytically involved in the first half-reaction of the enzyme (*i.e.* conversion of UDP-Glc to UDP-aldehydoglucose) (39, 42). Moreover, using Conseq analysis (freely available at the Internet site conseq.bioinfo.tau.ac.il/) (43), regions spanning from amino acids 41–54, 128–135, 340–350, and 461–464 have been identified as important for the structure or function of the protein (results not shown). Although this analysis is only a virtual prediction, it was done on all the known UGDH sequences deposited in the data bases. Such regions could be useful to understand not only the catalytic mechanism of the reaction but also to identify critical residues involved in a hypothetical regulatory mechanism that a pivotal enzyme such as UGDH could possess. Recently, for example, Conseq analysis has been successfully used to isolate important regions for protein-protein interactions (44).

Genomic Organization of xUGDH—By comparing the xUGDH transcript to the human and mouse genomic sequences available in public data bases, we have inferred the positions of the introns of the *xUGDH* gene. For each hypothetical intron, we have designed, on the two flanking exons, a pair of specific primers (Table 1) to amplify by long amplification PCR a region expected to contain the intron. PCR products were separated by gel electrophoresis, and the exon-intron junctions were sequenced. As reported in Table 2, top and bottom portions, the structure of the *xUGDH* gene is composed of 11 exons and 10 introns, and it matches that of mammalian *UGDH* genes (45). Notably, in the 5′-untranslated region of the human and mouse UGDH mRNA, we and others (45) found an additional intron of about 5700 bp. As this intron is located far upstream from the ATG start codon, we did not further investigate its position in the *xUGDH* gene. The major variability was detected in intron lengths, although all of them conserve their intron phase, indicating that the intron insertion points in the cDNA sequence have remained constant during *xUGDH* gene evolution. Most interestingly, the consensus gt-ag (5′–3′) splice site sequences are not always conserved in the *xUGDH* gene as shown in the 5′ splice acceptor sequence of intron 5. However, this noncanonical splice site has been reported to be quite frequent and does not cause any deleterious mutations (46, 47). Moreover, this noncanonical splice site may be the main 5′ intron acceptor site used during embryogenesis. In fact, no alternative splice isoforms of xUGDH transcripts have been found during *X. laevis* development by RT-PCR using two primers (*i.e.* xUGDH upper primer and xUGDH lower primer) flanking the intron 5 insertion point in the cDNA sequence.

X. laevis is certainly a well recognized "model organism" for cell and developmental biology, but it has the disadvantage of being tetraploid, which greatly complicates the creation of mutants and the analysis of gene regulation. In contrast, *X. tropicalis*, an amphibian of the same genus, is diploid and possesses a relatively small genome, whose sequencing is currently in progress. Therefore, *X. tropicalis* is destined to complement *X. laevis* as a model organism (26). Thanks to available preliminary data on the *X. tropicalis* genome (www.genome.jgipsf.org), we have determined the *X. tropicalis* UGDH genomic organization (Table 2, bottom portion), and as expected, the two genes are indeed very similar.

Recombinant xUGDH Expression and Characterization—To study the biochemical properties of xUGDH, we have generated the pHisx-UGDH plasmid that codes for a His_6-tagged xUGDH. This plasmid was used to transform *Escherichia coli* BL21(DE3)pLysS cells, and the recombinant protein expression was induced by IPTG treatment. Experiments were done to optimize the expression conditions, analyzing the effect of temperature, time of induction and collection, and IPTG concentration on xUGDH expression. The best conditions were obtained using *E. coli* cells grown overnight at 37 °C, induced with 1 mM IPTG, cultured at 30 °C, and harvested 24 h after induction. The recombinant xUGDH overexpressed under these conditions was completely soluble and thus fully recovered in the crude extract. The specific UGDH activity in the crude extract of induced *E. coli* BL21(DE3)pLysS was about 50-fold higher than that of crude extracts of uninduced cells (data not shown).

The crude extract from IPTG-induced *E. coli* cells was affinity-purified using a commercial spin column kit (Pierce). After the three elution steps suggested by the manufacturer, recombinant His-tagged xUGDH was eluted as a nearly single resolved band, and the final preparation was at least 90% homogeneous as judged by SDS-PAGE analysis (result not shown). The 54-kDa band corresponding to recombinant His-tagged xUGDH is in agreement with the molecular weight theoretically calculated from the translated xUGDH cDNA sequence. After the affinity chromatography step, the specific activity increased about 12-fold (data not shown).

As UGDH reduces two molecules of NAD to NADH during the conversion of a UDP-Glc substrate to a UDP-GlcUA, we followed the reaction by measuring NADH absorbance at 340 nm. To obtain kinetic

TABLE 2

Structure of the xUGDH gene

Top shows schematic representation of the xUGDH gene. Lines indicate introns; filled boxes indicate exons in the open reading frame; open boxes indicate exons in the 5′- and 3′-UTRs. Dotted lines and box represent the exon and the intron of the human UGDH gene located in the 5′-UTR (not characterized in the *X. laevis* gene). Bottom shows intron sizes were determined by gel electrophoresis, and position numbering is based on exon coding sequences where A of the ATG start codon is +1. Uppercase letters are exonic sequences, and lowercase letters are intronic sequences. n.d. indicate not determined. *Hs, Homo sapiens; Mm, Mus musculus; Xl, Xenopus laevis; Xt, Xenopus tropicalis.* Analyses were done on the basis of sequences AC021148 and AC108506 for human and mouse, respectively. The *X. tropicalis* UGDH genomic sequence was derived from sequence scaffold 10698, 7440, and AASO427206.bl.

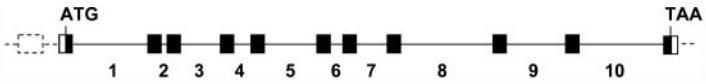

INTRON	SPECIE	EXON INTRON BOUNDARY SEQUENCE		LENGTH	PHASE	POSITION
1	*Hs*	ATTTATGAGgtaaacata	tctttttagCCAGGACTA	7166	0	162
	Mm	ATTTATGAGgtaaactat	cttctctagCCTGGATTA	1327	0	162
	Xt	ATTTATGAGgtaatggcc	tttttacagCCTGGGTTG	nd	0	162
	Xl	ATTTATGAGgtaatgacc	tcttcacagCCTGGGTTG	1700	0	162
2	*Hs*	TTTATTTCTgtaagtatt	ctacatcagGTGAATACT	3221	0	264
	Mm	TTTATTTCTgtaagtagt	tctcactagGTGAACACA	391	0	264
	Xt	TTTATCTCTgtaagtcgt	tattgacagGTCAACACT	87	0	264
	Xl	TTTATCTCTgtaagnctc	tcatttcagGTCAACACT	96	0	264
3	*Hs*	AATTTACAGgtataaaaa	ggattctagGTGCTGTCC	110	0	465
	Mm	AATTTACAGgtatgaaga	ctgttctagGTGCTGTCC	91	0	465
	Xt	AATTTACAGgtattaact	atctcacagGTGCTGTCT	297	0	465
	Xl	AATTTACAGgtaataact	ttctcacagGTGCTGTCT	1000	0	465
4	*Hs*	TCCAAACTGgttagtata	ttttttaagGCAGCAAAT	445	0	663
	Mm	TCCAAGCTGgtcagtgca	tctttaaagGCAGCCAAT	378	0	663
	Xt	TCAAAATTGgtatgagta	tggttgtagGCAGCCAAT	86	0	663
	Xl	TCAAAATTGgtatgagta	tggttgtagGCAGCCAAT	400	0	663
5	*Hs*	CCAGTGTTGgtaaattca	tttctgcagGGTTTGGTG	1099	1	811
	Mm	CCAGCGTTGgtaaaaaaa	ttccctcagGTTTTGGTG	2291	1	811
	Xt	CTAGTGTTGgtaatgaag	tttttatagGATTTGGTG	531	1	811
	Xl	CTAGTGTTGgtaaggcag	ataatagtgGATTTGGTG	1300	1	811
6	*Hs*	TGGCAGCAGgtattaatc	taatttcagGTCATAGAC	2816	0	906
	Mm	TGGCAGCAGgtatatatc	tattttcagGTCATAGAC	1640	0	906
	Xt	TGGCAACAGgtacaacat	ctgtgacagGTTATTGAT	448	0	906
	Xl	TGGCAACAGgtacaaaag	ccgtggtagGTTATTGAT	300	0	906
7	*Hs*	TGATACAAGgtatcagtt	ttcctatagAGAATCTTC	247	2	1037
	Mm	TGATACCAGgtacctgtt	gtccttcagAGAATCCTC	833	2	1037
	Xt	TGATACTAGgtaaatgaa	ttctattagAGAGTCTTC	426	2	1037
	Xl	TGATACTAGgtaaacaac	ttccatcagAGAATCTTC	750	2	1037
8	*Hs*	ATGACCAAGgtaaggctt	ttgttacagTGTCCCGGC	728	1	1171
	Mm	ATGACCAAGgtagggttg	tttttatagTGTCCAGAC	398	1	1171
	Xt	ATGACAGAGgtaatttat	ttcttacagTTTCCCAGC	905	1	1171
	Xl	ATGACAGAGgtaatactg	tacctgcagTGTCCCAGC	2300	1	1171
9	*Hs*	ATGTTTAAGgtaaggtaa	tctttacagGAATTGGAT	431	0	1263
	Mm	ATGTTTAAGgtgatgtag	tctacacagGAACTGGAT	85	0	1263
	Xt	ATGTTTAAGgtaatattg	gtcttgtagGAGTTGGAC	967	0	1263
	Xl	ATGTTTAAGgtaagcttg	gtcttgtagGAGCTGGAC	1400	0	1263
10	*Hs*	GGCTTCCAGgtaatcatg	ttttttcagATTGAAACA	3621	0	1374
	Mm	GGCTTCCAGgtaatcagg	tctcttcagATTGAAACA	2761	0	1374
	Xt	GGCTTCCAGgtaagtgag	tttttatagGTGGAAACC	nd	0	1374
	Xl	GGCTTTCAGgtaagtgag	tttttatagGTGGAAACC	2000	0	1374

constants (K_m and V_{max}) for substrate and cofactor, we used the same experimental buffers and conditions described previously (28). Moreover, we did not remove the His_6-tagged sequence as it has been reported that it does not alter the property of the enzyme (28). The purified enzyme showed no reduction of NAD if incubated with either UDP-galactose, UDP-GlcUA, or UDP-N-acetylglucosamine, indicating the purity and specificity of the enzyme (results not shown).

The steady-state kinetic parameters of His-tagged xUGDH have been calculated by incubating the enzyme with increasing concentrations of NAD in the presence of saturating UDP-Glc substrate (Fig. 1*A*). Similarly, the dependence of reaction kinetics on the substrate was measured by increasing UDP-Glc concentration in the presence of saturating NAD (Fig. 1*C*). For both the substrates, saturation kinetics were observed. A double-reciprocal plot of the initial velocities revealed a K_m of 0.9 mM for UDP-Glc (Fig. 1*B*) and a K_m of 0.3 mM for NAD (Fig. 1*D*). Both sets of conditions yielded a similar V_{max} of about 10 nmol of NADH/min/mg of enzyme. These data are comparable with those of UGDH from other species (Table 3).

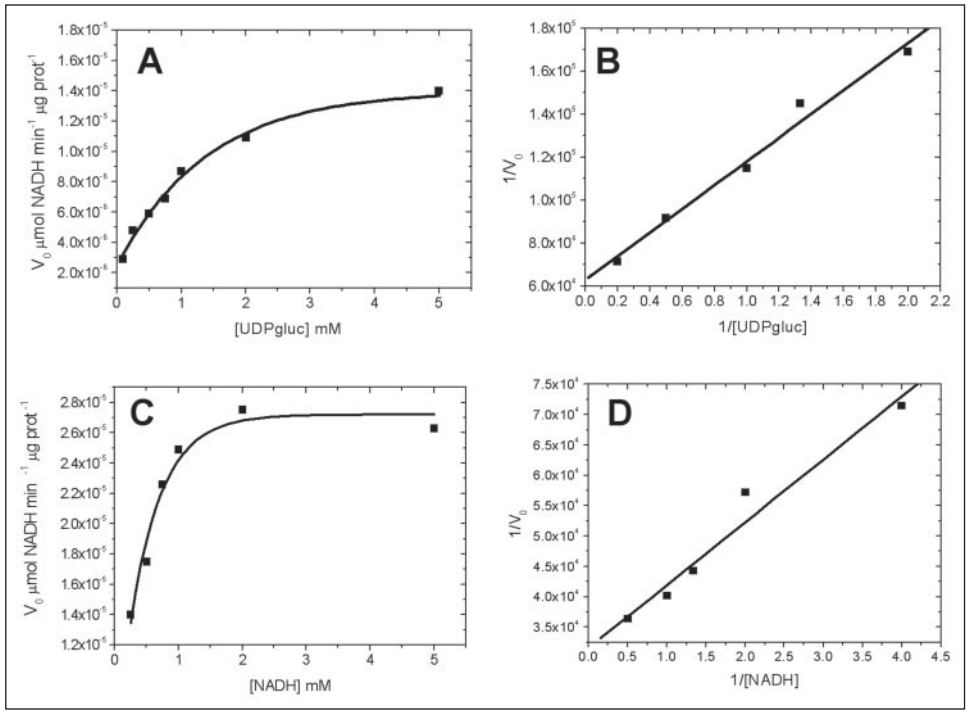

FIGURE 1. Kinetics of xUGDH using a variable amount of UGDH with a saturation quantity of NAD (10 mM) (*A*) or variable amounts of NAD with a saturation quantity of UGDH (5 mM) (*C*). K_m values for UGDH and NAD were calculated by the Lineweaver-Burk method for data shown in *B* and *D*, respectively. Thirty micrograms of purified xUGDH were used for each determination. The plots represent the mean of three independent experiments.

TABLE 3
Comparison of K_m values (expressed in mM) of UGDH from different species

Species	K_m		Ref.
	NAD	UDP-Glc	
X. laevis	0.3	0.9	This work
Homo sapiens	0.35	0.1	28
Gallus gallus	0.9	0.5	33
C. elegans	0.2	0.2	13
E. coli	1	0.05	48
Streptococcus pyogenes	0.06	0.02	64

xUGDH Expression during Development—The amphibian *X. laevis* has become one of the most studied organisms in developmental biology together with *C. elegans* and *D. melanogaster*. As no information was available, we investigated the regulation of xUGDH during *X. laevis* development. RT-PCR was done on RNA extracted from the same number of embryos at different developmental stages. To visualize differences in the expression, different PCR cycles were done as outlined in Fig. 2. Although the 531-bp-long band corresponding to the amplicon of xUGDH was detectable in all the tested developmental stages, a more pronounced signal was visualized in the sample from 30 h post-fertilization (hpf) that corresponds to an embryo at the tail bud stage. Such an expression pattern is related to the crucial function of UDP-GlcUA. In fact, this molecule is a precursor for all GAGs (with the exception of keratan sulfate), including GAGs of proteoglycans and HA that are known to be essential for a proper development (11). Most interestingly, the increase in xUGDH in the 30-hpf embryos corresponded with our previous finding that HA is dramatically elevated in embryos at this developmental stage (34). Moreover, the enzymes involved in HA synthesis (*i.e.* HAS2 and HAS3) are also up-regulated in this embryonic stage (34). Although the precise role of HA in *X. laevis* development is still to be defined, HA is critical during embryonic development of mammals. For example, mice unable to produce HA die in the uterus from severe cardiac malformation (49, 50).

xUGDH Expression and HA Synthesis—The data reported in this study strongly support the hypothesis that coordinated expression of

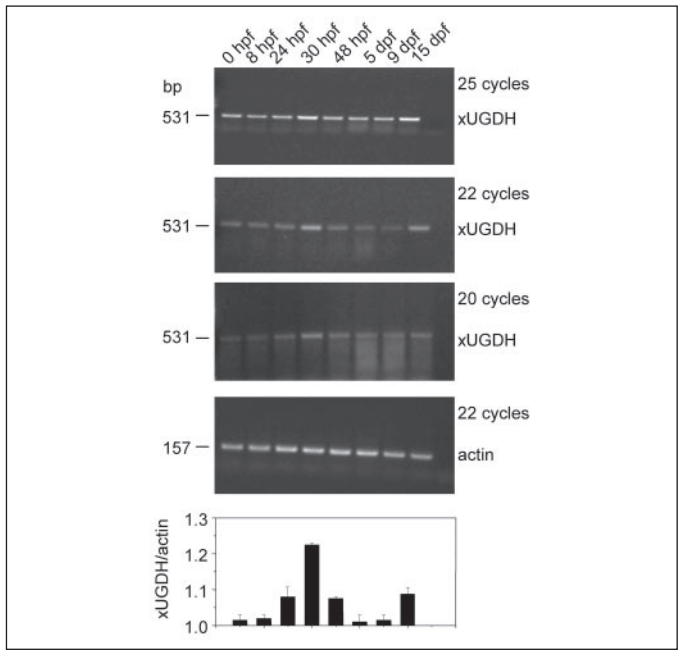

FIGURE 2. **Expression of the mRNAs coding for xUGDH during embryogenesis at the indicated hpf or days post-fertilization (*dpf*).** Different RT-PCR cycles were used to visualize an increase in xUGDH expression at 30 hpf. Cytoskeletal actin was used as a reference. *Bottom panel*, quantitative densitometric analysis (mean ± S.D.) of gels from two independent experiments. xUGDH:β-actin ratio at 0 hpf was fixed as 1.

UGDH and HAS may have a pivotal role in regulating HA levels. To elucidate the relationship between UGDH and HA synthesis and accumulation, we transfected human primary aortic smooth muscle cells (AoSMCs) with an xUGDH expression plasmid pTarget-xUGDH-sense. We also transfected the plasmid pTarget-xUGDH-antisense that did not code for any protein as a control. We hypothesized that an increase in UGDH activity that augments UDP-GlcUA synthesis may increase the synthesis of HA. As shown in Fig. 3*A*, UGDH activity increased in AoSMCs transfected with pTarget-xUGDH-sense,

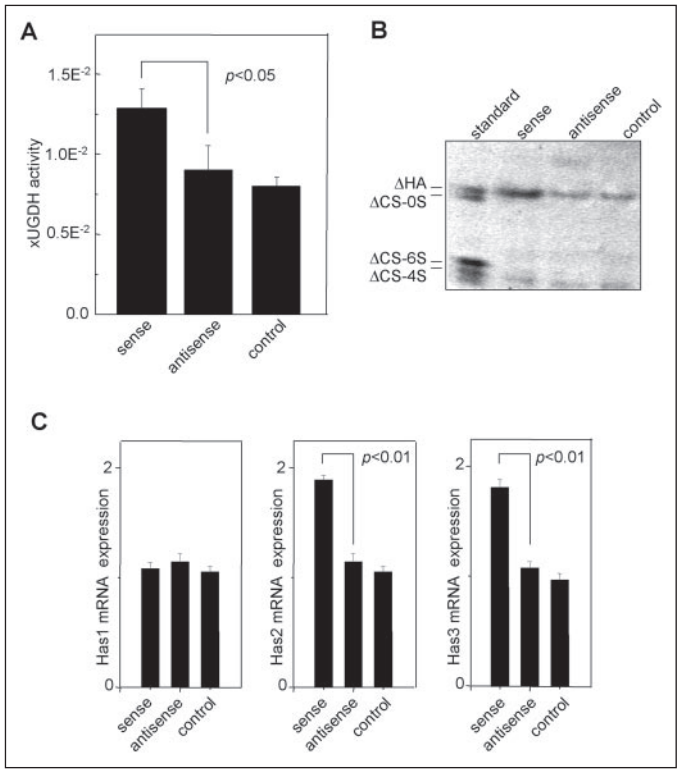

FIGURE 3. *A,* UGDH activities in AoSMC extracts transfected with pTarget-xUGDH-sense (*sense*), pTarget-xUGDH-antisense (*antisense*), or without DNA (*control*). xUGDH activities are expressed in mmol of NADH min^{-1} mg $protein^{-1}$. Transfections were done in triplicate, and data are expressed as means ± S.E. *B,* FACE analyses on conditioned culture media of AoSMCs transfected as described above. Δ*HA*, HA disaccharide; Δ*CS-0S*, chondroitin disaccharide; Δ*CS-4S*, chondroitin 4-sulfated disaccharide; Δ*CS-6S*, chondroitin 6-sulfated disaccharide. The analyses were done in triplicate, and one representative result is shown. *C,* quantification of mRNA coding for HAS1, HAS2, and HAS3 by RT-PCR in AoSMCs transfected with pTarget-xUGDH-sense (*sense*), pTarget-xUGDH-antisense (*antisense*), or without DNA (*control*) after 48 h of incubation. Transfections for gene expression analyses and the quantifications were repeated three times with identical results both using β-actin (shown) or glyceraldehyde-3-phosphate dehydrogenase (*GAPDH*) (not shown) as reference genes. Unpaired Student's *t* test was performed for statistical analyses using Origin 7.5 software (Microcal Software). Gene expression is expressed in arbitrary units.

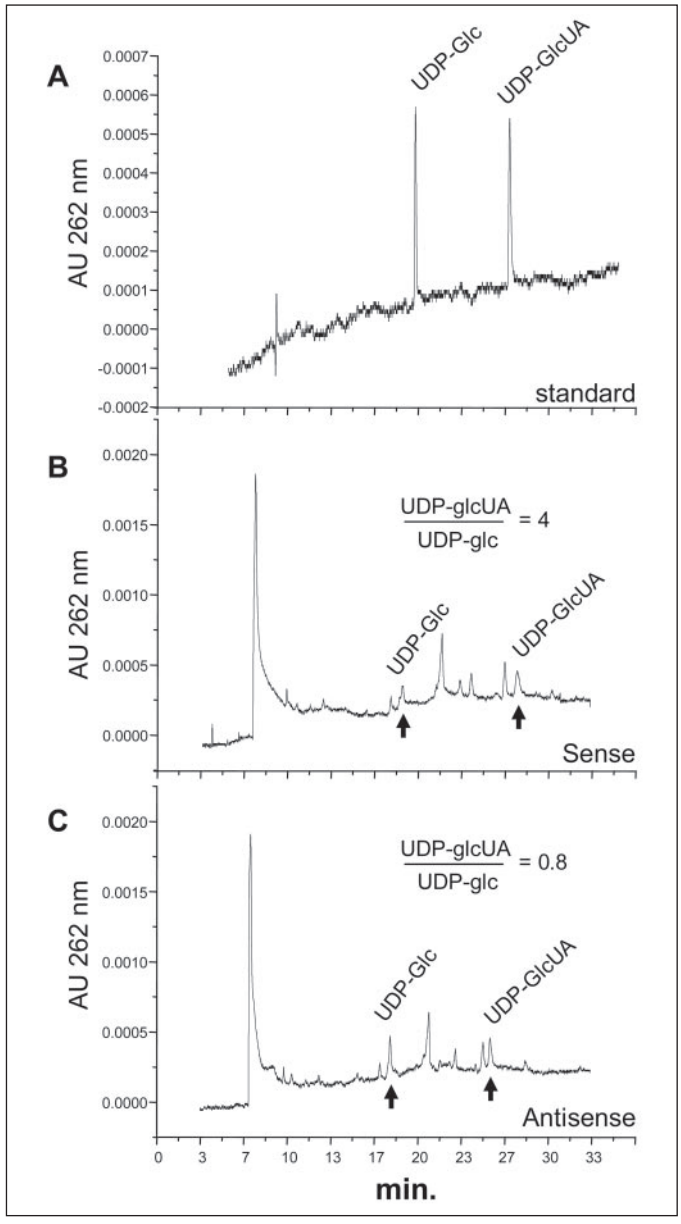

FIGURE 4. **Capillary zone electropherogram showing the UDP-Glc and UDP-GlcUA separations.** *A,* separation of standard (70 μM) of UDP-Glu and UDP-GluA in 90 mM borate buffer, pH 9. *B,* separation of extracts from AoSMC transfected with pTarget-xUGDH-sense vector. *C,* separation of extracts from AoSMC transfected with pTarget-xUGDH-antisense vector. AoSMC extracts were prepared after 48 h from transfection. In the cellular extracts, *arrows* precisely indicate the UDP-Glc and UDP-GlcUA peaks.

whereas cells transfected with pTarget-xUGDH-antisense maintained a lower UGDH activity comparable with that of untransfected cells. The increment of UGDH activity of pTarget-xUGDH-sense transfected cells was in agreement with that reported for other mammalian cell lines transfected with mouse or bovine UGDH (42, 51). To verify that a UGDH activity increase could actually increase UDP-GlcUA, we quantified the UDP-GlcUA:UDP-Glc ratio by capillary zone electrophoresis (Fig. 4). AoSMCs transfected with pTarget-xUGDH-sense, pTarget-xUGDH-antisense vectors, or not transfected showed UDP-GlcUA: UDP-glucose ratios of 4, 0.8, and 0.7, respectively. This clearly indicates that the increase of UGDH activity augmented the cellular UDP-GlcUA levels by about 4-fold with respect to control levels.

The conditioned culture media of the AoSMC cultures were collected after 48 h of transfection, and their HA concentrations were measured by FACE analysis (Fig. 3*B*). AoSMCs produce high levels of HA (52, 53). Most interestingly, the HA disaccharide band derived from 10^6 pTarget-xUGDH-sense transfected AoSMCs was significantly stronger than that derived from the same number of control cells (*i.e.* transfected with pTarget-xUGDH-antisense or not transfected). The UGDH activity detected in control cells (Fig. 3*A*) could explain the basal HA signals in control cell culture medium (Fig. 3*B*). On the other hand, the increase of HA production in pTarget-xUGDH-sense transfected cells could be ascribed to the augmented UGDH activity in those cells. A similar result was obtained by Magee *et al.* (54) who discovered that the up-regulation of UDP-glucose pyrophosphorylase stimulates HA synthesis in hypertrophic chondrocyte cultures. As UDP-glucose pyrophosphorylase and UGDH belong to the same pathway that forms UDP-GlcUA, it would be reasonable that the up-regulation of both of these enzymes can increase the concentration of HA synthesis precursors. Moreover, the K_m values of the three HA synthases are in the range of the cytoplasmic concentration of UDP-sugars (55), making the activity of HA synthetic enzymes responsive to the concentrations and the pool sizes of the cellular sugar nucleotides.

Most interestingly, densitometric quantification of the HA and the chondroitin 4-sulfate disaccharide bands obtained from FACE analyses revealed that chondroitin 4-sulfate synthesis did not change significantly after the xUGDH transfections (results not shown), indicating

that the UGDH effect was selective for HA. Although UGDH is a central enzyme in the metabolism of GAGs, it may specifically regulate HA accumulation without altering other GAGs. In light of this specific HA increase, we performed quantitative RT-PCR analyses on transfected AoSMC cDNA and found that HAS2 and HAS3 mRNA levels were up-regulated about 2-fold only in pTarget-xUGDH-sense transfected cells, whereas HAS1 mRNA levels were unchanged (Fig. 3*C*). This suggests that transfection of UGDH leads to an induction of *HAS2* and *HAS3* gene transcription or to a stabilization of HAS2 and HAS3 mRNAs. The specific increase of HAS2 and HAS3 fits well with the specific increase of HA in transfected AoSMCs (Fig. 3*B*).

The lack of increase in chondroitin sulfate may result from the fact that precursors for this GAG must enter the Golgi apparatus by using several UDP-sugar transporters that have been shown to possess low K_m values for their substrates (*i.e.* 1–10 μM) (56, 57). Although cytoplasmic UDP-sugar precursor concentrations could directly affect the activity of HA synthases located in the cell membrane, the UDP-sugar transporters would be saturated at the cellular concentration of the UDP-sugar precursors thereby maintaining constant concentrations inside the Golgi apparatus and thus the constant activity of the Golgi GAG synthetic enzymes. The tight relationship between UGDH activity and GAG synthesis was also recently outlined in *in vivo* experiments with fibroblast-like synovial lining cells (58) and *in vitro* on immature and mature human articular cartilage explants (59), although the key importance of UGDH activity in GAG production was already suggested years ago (60, 61).

Abrogation of Human UGDH and HA Synthesis—To demonstrate the putative link between UGDH activity and HA synthesis, we did siRNA experiments to reduce the endogenous UGDH in human AoSMCs. The greatest reduction of human UGDH mRNA was achieved by transfecting 50 μM of UGDH siRNA and incubating for 48 h. In these conditions quantitative RT-PCR showed a reduction of the human UGDH transcript of about 90% with respect to the controls (*i.e.* scramble siRNA and no DNA transfected cells) (Fig. 5*A*). Such a reduction of UGDH mRNA corresponded to a strong inhibition of UGDH activity. In fact, we were not able to detect any signals in the UGDH spectrophotometric assay used in this work indicating that the residual UGDH activity was below the detection limit of the assay (result not shown). To verify that the UGDH activity decrease could actually reduce UDP-GlcUA content, we quantified the UDP-GlcUA:UDP-Glc ratios (data not shown). AoSMCs transfected with UGDH siRNA, scramble siRNA, or not transfected showed UDP-GlcUA:UDP-glucose ratios of 0.25, 1.0, and 0.8, respectively, clearly indicating that the inhibition of UGDH activity reduced the cellular UDP-GlcUA levels by 4-fold with respect to control levels. Furthermore, the concentrations of HA in the conditioned culture media clearly showed a corresponding decrease (Fig. 5*B*) indicating that HA synthesis could be strictly regulated by the availability of the UDP-sugar precursors at least in AoSMCs. This finding supports the proposed mechanism of the 4-methylumbelliferone inhibition of HA synthesis; in fact, the glucuronidation of 4-methylumbelliferone by endogenous UDP-glucuronyltransferase induces a depletion of UDP-GlcUA (62). Moreover, chondroitin 4-sulfate was not influenced by changing availability of the precursors (see above).

Most interestingly, the inhibition of UGDH by siRNA did not change the levels of transcripts coding for HAS1, HAS2, and HAS3 quantified by quantitative RT-PCR (Fig. 5*C*). These data indicated that the expression of these enzymes cannot be reduced below a basal level even when one of their substrates is strongly decreased.

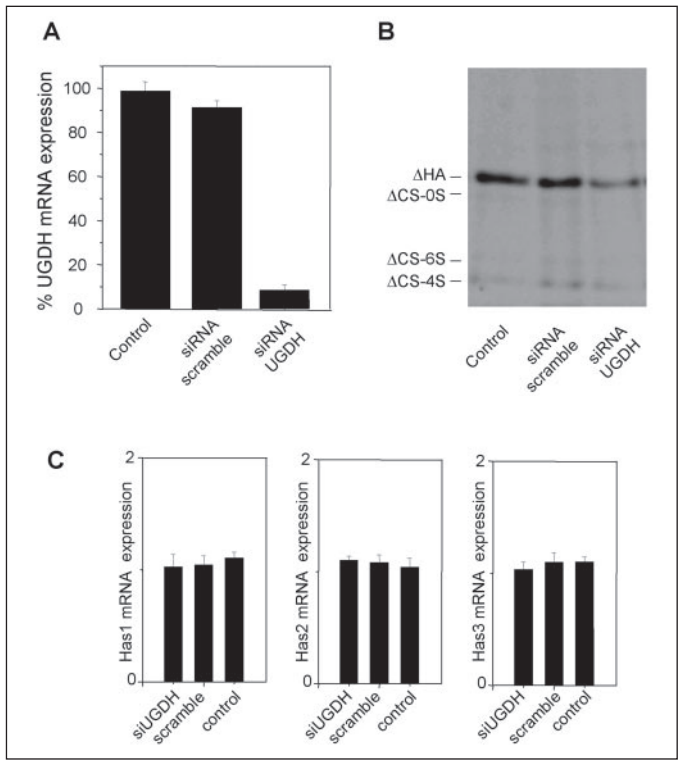

FIGURE 5. *A,* UGDH mRNA quantification by RT-PCR in AoSMCs transfected with no siRNA (*control*), a scramble siRNA (*scramble*), or siRNA against human UGDH (*siUGDH*). Transfections were done in triplicate, and data are expressed as means ± S.E. *B,* FACE analyses of conditioned culture media of siRNA AoSMCs transfected as described above (see Fig. 3 legend for disaccharides designations). The analyses were done in triplicate, and one representative result is shown. *C,* quantification of mRNA coding for HAS1, HAS2, and HAS3 by quantitative RT-PCR in AoSMCs transfected with no siRNA (*control*), a scramble siRNA (*scramble*), or siRNA against human UGDH (*siUGDH*). Transfections for gene expression analyses and the quantification were repeated three times with identical results using both β-actin (shown) or glyceraldehyde-3-phosphate dehydrogenase (not shown) as reference genes. Gene expression is expressed in arbitrary units.

GAG Determinations—To better elucidate the UGDH role in the control of GAG synthesis, we incubated AoSMCs with [^{3}H]glucosamine to determine the GAG amount. We found that the total (*i.e.* medium and cell layer) incorporated radioactivity associated with GAGs was much higher in pTarget-xUGDH-sense transfected cells than in the controls (*i.e.* 0.16 *versus* 0.12 cpm/cell, respectively). On the other hand, the incorporated radioactivity associated with GAGs was lower in siRNA against UGDH-treated cells than in the controls (0.06 *versus* 0.12 cpm/cell, respectively). The silencing of UGDH affected dramatically the GAG associated to the cell layer fractions in which the radioactivity incorporated in the GAG was undetectable. These data support the critical role of UGDH in promoting GAG synthesis.

Moreover, we quantified the percentage of the specific GAG family in conditioned medium (Table 4) as well as the cell layer (Table 5) samples. The determinations were performed counting the radioactivity in GAG resistant to hyaluronidase SD, chondroitinase ABC, and heparinase I, II, and III digestions as described under "Materials and Methods." For the percentage calculations, the total radioactivity that was digested was considered 100%. The quantifications were done on untransfected AoSMCs (Tables 4 and 5, control row) or transfected with pTarget-xUGDH-sense (Tables 4 and 5, sense row) or with siRNA against human UGDH (Tables 4 and 5, RNA UGDH row). We found that HA is the most produced GAG in the medium as well as in the cell layer. Most interestingly, when we overexpressed the xUGDH, we found a significant increase in both medium and cell-associated HA content, whereas the synthesis of other GAGs was only slightly modified (Tables 4 and 5).

TABLE 4

Conditioned medium GAG content in AoSMCs

AoSMCs (control) or AoSMCs transfected with either pTarget-xUGDH-sense (sense) or pTarget-xUGDH-antisense (antisense), scramble siRNA (scramble) or siRNA against human UGDH (siRNA UGDH) were treated as outlined under "Materials and Methods." GAG contents are reported in percent of the total radioactivity digested in the sample. The total GAG column represents the percentage of the total radioactivity sensitive to enzymatic digestions. The reported data are the mean of two independent experiments.

	ΔHeparan sulfate medium	ΔChondroitin sulfate medium	ΔHeparan sulfate medium	Total GAG %
Control	77	13	9	99
Sense	83	9	7	99
Antisense	78	13	9	100
siRNA scramble	79	12	8	99
siRNA UGDH	68	14	10	92

TABLE 5

Cell-associated GAG content in AoSMCs

AoSMCs (control) or AoSMCs transfected with either pTarget-xUGDH-sense (sense) or pTarget-xUGDH-antisense (antisense), scramble siRNA (scramble) or siRNA against human UGDH (siRNA UGDH) were treated as outlined under "Material and Methods." GAG contents are reported in percent of the total radioactivity in the sample. Nd indicates not detected. The total GAG column represents the percentage of the total radioactivity sensitive to enzymatic digestions. The reported data are the mean of two independent experiments.

	ΔHeparan sulfate cell	ΔChondroitin sulfate cell	ΔHeparan sulfate cell	Total GAG %
Control	40	6	30	76
Sense	62	8	27	97
Antisense	44	5	30	79
siRNA scramble	43	6	30	79
siRNA UGDH	nd	nd	nd	0

On the other hand, when we abolished the expression of UGDH in AoSMC by siRNA, we found a decrease of medium HA without altering the synthesis of other released GAGs. However, in the cell layer-associated GAGs, the incorporated radioactivity was under the detection limit (Tables 4 and 5), indicating that cell surface-associated GAGs could have a more rapid turnover in comparison to GAGs secreted into the medium. Most interestingly, as the sum of percentages indicated in the table rows represents the GAG-associated radioactivity, it is noteworthy that in the medium fractions almost 100% of the radioactivity was GAG-associated, and in the cell fractions the radioactivity accounted for about 80%. This value reached about 100% when UGDH was induced, and this increase (~20%) was specifically caused by HA synthesis.

As observed from our previous results (Figs. 3*B* and 5*B*), we showed that HA is the GAG that is more sensitive to UDP-GlcUA concentration inside the cytoplasm, and therefore, the cell could regulate specifically the HA synthesis controlling the UDP-GlcUA availability.

In Vivo xUGDH Silencing—X. laevis embryos were injected bilaterally with xUGDH MO complementary to the 5′-UTR of xUGDH mRNA to prevent its translation. Control and xUGDH MO-treated embryos were co-injected with mRNA coding for the green fluorescent protein (GFP), allowing the selection of only those embryos injected in both sides, before the subsequent analysis. Embryos treated with xUGDH MO had severe malformations at the end of gastrulation that led to a failure in the blastopore closure. In the subsequent developmental phases, xUGDH MO-injected embryos are not able to complete the neurulation step correctly as the neural tube remained posteriorly opened (90% of injected embryos $n = 120$) (Fig. 6*A*). In contrast control embryos (injected with the same dose of the 5-mismatch MO) showed a normal development (100% of injected embryos $n = 130$) (Fig. 6*B*). The embryos progressively died and did not reach the tail bud stage. It has been shown that during gastrulation, both in *X. laevis* and mouse embryos, mesodermal cells enter and move within an HA-rich environment (23, 63). Moreover, the HAS2 is expressed in the involuting mesoderm in *X. laevis* embryos (35) and appears to be critical in the Zebrafish gastrulation process (32). Therefore, our xUGDH knock down functional data are consistent with a role of HA in the gastrulation movements and suggest an important role of the xUGDH activity during early *X. laevis* development.

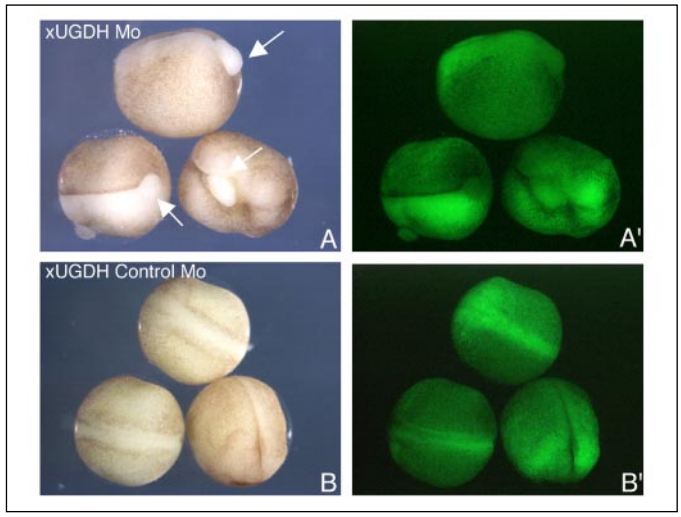

FIGURE 6. **xUGDH down-regulation during early *X. laevis* development.** *A,* dorsal view of representative *X. laevis* embryos at late neurula stage (20 hpf) injected with xUGDH Mo. The neural tubes remain posteriorly opened as indicated by the *arrows*. Control embryos at the same developmental stage, injected with the control morpholino (xUGDH mismatched oligonucleotide), have normally completed the neurulation step and are shown in *B*. The distribution of the injected morpholino-oligonucleotides is visualized by GFP fluorescence as shown in *A′* and *B′*.

In conclusion, we have reported the cloning of the UGDH cDNA sequence from the amphibian *X. laevis,* and we found that the gene structure and biochemical properties confirmed the data obtained in other species. We described an up-regulation of xUGDH mRNA during the tail bud stage of *X. laevis* development that was correlated with the elevated HA production typical of the developing embryo at this stage. We also demonstrated a critical role of xUGDH activity in *Xenopus* early development. Functional down-regulation of xUGDH, in fact, results in early embryonic lethality. Moreover, we reported that an increase in UGDH may be responsible for HA accumulation at least in an *in vitro* cellular model. These results support the hypothesis that the synthesis of HA requires the activation of a complex mixture of enzymes, not only the synthetic proteins but also the enzymes involved in metabolism of the UDP-sugar precursors.

Acknowledgments—We thank Edward Maytin for critical discussion of the manuscript and Prof. Robert H. Horvitz and Erik Andersen for anti-C. elegans UDP-glucose dehydrogenase (SQV-4) antibodies that unfortunately do not recognize the X. laevis *enzyme. We also thank Paola Moretto, Pierangelo Borroni, and Kostantinos Sideris for technical assistance. We acknowledge the "Centro Grandi Attrezzature per la Ricerca Biomedica" Università degli Studi dell'Insubria, for the availability of needed instruments.*

REFERENCES

1. Oppenheimer, N. J., and Handlon, A. L. (1992) *Enzymes* **20,** 453–504
2. Roden, L. (1980) in *The Biochemistry of Glycoproteins and Proteoglycans* (Lennarz, W. J., ed) Plenum Publishing Corp., New York
3. Dutton, G. J. (1980) *Glucuronidation of Drugs and Other Compounds*, CRC Press Inc, Boca Raton, FL
4. D'Alessandro, G., and Northcote, D. H. (1977) *Biochem. J.* **162,** 281–288
5. Arrecubieta, C., Lopez, R., and Garcia, E. (1994) *J. Bacteriol.* **176,** 6375–6383
6. Dougherty, B. A., and van de Rijn, I. (1993) *J. Biol. Chem.* **268,** 7118–7124
7. Ge, X., Penney, L. C., van de Rijn, I., and Tanner, M. E. (2004) *Eur. J. Biochem.* **271,**

14–22
8. Iozzo, R. V., and San Antonio, J. D. (2001) *J. Clin. Investig.* **108,** 349–355
9. Selva, E. M., and Perrimon, N. (2001) *Adv. Cancer Res.* **83,** 67–80
10. Toole, B. P., Wight, T. N., and Tammi, M. I. (2002) *J. Biol. Chem.* **277,** 4593–4596
11. Princivalle, M., and de Agostini, A. (2002) *Int. J. Dev. Biol.* **46,** 267–278
12. Hacker, U., Lin, X., and Perrimon, N. (1997) *Development* (*Camb.*) **124,** 3565–3573
13. Hwang, H. Y., and Horvitz, H. R. (2002) *Proc. Natl. Acad. Sci. U. S. A.* **99,** 14224–14229
14. Hwang, H. Y., Olson, S. K., Esko, J. D., and Horvitz, H. R. (2003) *Nature* **423,** 439–443
15. Walsh, E. C., and Stainier, D. Y. (2001) *Science* **293,** 1670–1673
16. Garcia-Garcia, M. J., and Anderson, K. V. (2003) *Cell* **114,** 727–737
17. Galli, A., Roure, A., Zeller, R., and Dono, R. (2003) *Development* (*Camb.*) **130,** 4919–4929
18. Latinkic, B. V., Mercurio, S., Bennett, B., Hirst, E. M., Xu, Q., Lau, L. F., Mohun, T. J., and Smith, J. C. (2003) *Development* (*Camb.*) **130,** 2429–2441
19. Sander, V., Mullegger, J., and Lepperdinger, G. (2001) *Mech. Dev.* **102,** 251–253
20. Anderson, R. B., Walz, A., Holt, C. E., and Key, B. (1998) *Dev. Biol.* **202,** 235–243
21. Somasekhar, T., and Nordlander, R. H. (1997) *Dev. Brain Res.* **99,** 208–215
22. Grunz, H., and Tacke, L. (1990) *Cell Differ. Dev.* **32,** 117–123
23. Mullegger, J., and Lepperdinger, G. (2002) *Mol. Reprod. Dev.* **61,** 312–316
24. Koprunner, M., Mullegger, J., and Lepperdinger, G. (2000) *Mech. Dev.* **90,** 275–278
25. Haddon, C. M., and Lewis, J. H. (1991) *Development* (*Camb.*) **112,** 541–550
26. Beck, C. W., and Slack, J. M. (2001) *Genome Biol.* http://genomebiology.com/2001/2/10/reviews/1029
27. Sambrook, J., Fritsch, E. F., and Maniatis, T. (1989) *Molecular Cloning: A Laboratory Manual,* Cold Spring Harbor Laboratory Press, Cold Spring Harbor, NY
28. Sommer, B. J., Barycki, J. J., and Simpson, M. A. (2004) *J. Biol. Chem.* **279,** 23590–23596
29. Vigetti, D., Monetti, C., Pollegioni, L., Taramelli, R., and Bernardini, G. (2000) *Arch. Biochem. Biophys.* **379,** 90–96
30. Karousou, E. G., Militsopoulou, M., Porta, G., De Luca, G., Hascall, V. C., and Passi, A. (2004) *Electrophoresis* **25,** 2919–2925
31. Lehmann, R., Huber, M., Beck, A., Schindera, T., Rinkler, T., Houdali, B., Weigert, C., Haring, H. U., Voelter, W., and Schleicher, E. D. (2000) *Electrophoresis* **21,** 3010–3015
32. Bakkers, J., Kramer, C., Pothof, J., Quaedvlieg, N. E., Spaink, H. P., and Hammerschmidt, M. (2004) *Development* (*Camb.*) **131,** 525–537
33. Bdolah, A., and Feingold, D. S. (1968) *Biochim. Biophys. Acta* **159,** 176–178
34. Vigetti, D., Viola, M., Gornati, R., Ori, M., Nardi, I., Passi, A., De Luca, G., and Bernardini, G. (2003) *Matrix Biol.* **22,** 511–517
35. Nardini, M., Ori, M., Vigetti, D., Gornati, R., Nardi, I., and Perris, R. (2004) *Gene Expression Patterns* **4,** 303–308
36. Mijakovic, I., Poncet, S., Boel, G., Maze, A., Gillet, S., Jamet, E., Decottignies, P., Grangeasse, C., Doublet, P., Le Marechal, P., and Deutscher, J. (2003) *EMBO J.* **22,** 4709–4718
37. Grangeasse, C., Obadia, B., Mijakovic, I., Deutscher, J., Cozzone, A. J., and Doublet, P. (2003) *J. Biol. Chem.* **278,** 39323–39329
38. Campbell, R. E., Mosimann, S. C., van de Rijn, I., Tanner, M. E., and Strynadka, N. C. (2000) *Biochemistry* **39,** 7012–7023
39. Johansson, H., Sterky, F., Amini, B., Lundeberg, J., and Kleczkowski, L. A. (2002) *Biochim. Biophys. Acta* **1576,** 53–58
40. Perozich, J., Leksana, A., and Hempel, J. (1995) *Adv. Exp. Med. Biol.* **372,** 79–84
41. Hempel, J., Perozich, J., Romovacek, H., Hinich, A., Kuo, I., and Feingold, D. S. (1994) *Protein Sci.* **3,** 1074–1080
42. Spicer, A. P., Kaback, L. A., Smith, T. J., and Seldin, M. F. (1998) *J. Biol. Chem.* **273,** 25117–25124
43. Berezin, C., Glaser, F., Rosenberg, J., Paz, I., Pupko, T., Fariselli, P., Casadio, R., and Ben Tal, N. (2004) *Bioinformatics.* **20,** 1322–1324
44. Torrado, M., Nespereira, B., Lopez, E., Centeno, A., Castro-Beiras, A., and Mikhailov, A. T. (2005) *J. Mol. Cell. Cardiol.* **38,** 353–365
45. Bontemps, Y., Maquart, F. X., and Wegrowski, Y. (2000) *Biochem. Biophys. Res. Commun.* **275,** 981–985
46. Burset, M., Seledtsov, I. A., and Solovyev, V. V. (2000) *Nucleic Acids Res.* **28,** 4364–4375
47. Burset, M., Seledtsov, I. A., and Solovyev, V. V. (2001) *Nucleic Acids Res.* **29,** 255–259
48. Schiller, J. G., Bowser, A. M., and Feingold, D. S. (1973) *Biochim. Biophys. Acta* **293,** 1–10
49. Camenisch, T. D., Schroeder, J. A., Bradley, J., Klewer, S. E., and McDonald, J. A. (2002) *Nat. Med.* **8,** 850–855
50. Camenisch, T. D., Spicer, A. P., Brehm-Gibson, T., Biesterfeldt, J., Augustine, M. L., Calabro, A., Jr., Kubalak, S., Klewer, S. E., and McDonald, J. A. (2000) *J. Clin. Investig.* **106,** 349–360
51. Lind, T., Falk, E., Hjertson, E., Kusche-Gullberg, M., and Lidholt, K. (1999) *Glycobiology* **9,** 595–600
52. Evanko, S. P., Angello, J. C., and Wight, T. N. (1999) *Arterioscler. Thromb. Vasc. Biol.* **19,** 1004–1013
53. Ye, L., Mora, R., Akhayani, N., Haudenschild, C. C., and Liau, G. (1997) *Circ. Res.* **81,** 289–296
54. Magee, C., Nurminskaya, M., and Linsenmayer, T. F. (2001) *Biochem. J.* **360,** 667–674
55. Itano, N., Sawai, T., Yoshida, M., Lenas, P., Yamada, Y., Imagawa, M., Shinomura, T., Hamaguchi, M., Yoshida, Y., Ohnuki, Y., Miyauchi, S., Spicer, A. P., McDonald, J. A., and Kimata, K. (1999) *J. Biol. Chem.* **274,** 25085–25092
56. Berninsone, P., Hwang, H. Y., Zemtseva, I., Horvitz, H. R., and Hirschberg, C. B. (2001) *Proc. Natl. Acad. Sci. U. S. A.* **98,** 3738–3743
57. Hoflich, J., Berninsone, P., Gobel, C., Gravato-Nobre, M. J., Libby, B. J., Darby, C., Politz, S. M., Hodgkin, J., Hirschberg, C. B., and Baumeister, R. (2004) *J. Biol. Chem.* **279,** 30440–30448
58. Pitsillides, A. A. (2003) *Cell Biochem. Funct.* **21,** 235–240
59. Hickery, M. S., Bayliss, M. T., Dudhia, J., Lewthwaite, J. C., Edwards, J. C., and Pitsillides, A. A. (2003) *J. Biol. Chem.* **278,** 53063–53071
60. Molz, R. J., and Danishefsky, I. (1971) *Biochim. Biophys. Acta* **250,** 6–13
61. Balduini, C., Brovelli, A., De Luca, G., Galligani, L., and Castellani, A. A. (1973) *Biochem. J.* **133,** 243–249
62. Kakizaki, I., Kojima, K., Takagaki, K., Endo, M., Kannagi, R., Ito, M., Maruo, Y., Sato, H., Yasuda, T., Mita, S., Kimata, K., and Itano, N. (2004) *J. Biol. Chem.* **279,** 33281–33289
63. Fenderson, B. A., Stamenkovic, I., and Aruffo, A. (1993) *Differentiation* **54,** 85–98
64. Campbell, R. E., Sala, R. F., van de Rijn, I., and Tanner, M. E. (1997) *J. Biol. Chem.* **272,** 3416–3422